Journal of Electroanalytical Chemistry 691 (2013) 77–82

Contents lists available at SciVerse ScienceDirect

Journal of Electroanalytical Chemistry

journal homepage: www.elsevier.com/locate/jelechem

Electrochemical characterization of sub-micro-gram amounts of organic semiconductors using scanning droplet cell microscopy

Jacek Gasiorowski [a], Andrei I. Mardare [b], Niyazi S. Sariciftci [a], Achim Walter Hassel [b,*]

[a] Linz Institute for Organic Solar Cells (LIOS), Physical Chemistry, Johannes Kepler University, Linz, Austria
[b] Institute for Chemical Technology of Inorganic Materials, Johannes Kepler University, Linz, Austria

ARTICLE INFO

Article history:
Received 5 September 2012
Received in revised form 5 November 2012
Accepted 7 November 2012
Available online 1 December 2012

Keywords:
Scanning droplet cell microscopy
Organic semiconductors
Electrochemical impedance spectroscopy

ABSTRACT

Scanning droplet cell microscopy (SDCM) uses a very small electrolyte droplet at the tip of a capillary which comes in contact with the working electrode. This method is particularly interesting for studies on organic semiconductors since it provides localized electrochemical investigations with high reproducibility. One clear advantage of applying SDCM is represented by the very small amounts of material necessary (less than 1 mg). Organic materials can be investigated quickly and inexpensively in electrochemical studies with a high throughput. In the present study, thin layers of poly(3-hexylthiophene) (P3HT), which is one of the most often used material for organic solar cells, were deposited on ITO/glass as working electrodes in SDCM studies. The redox reactions in 0.1 M tetra(n-butyl)ammonium hexafluorophosphate ($TBAPF_6$) dissolved in propylene carbonate were studied by cyclic voltammetry and by electrochemical impedance spectroscopy. Two reversible, distinct oxidation steps of the P3HT were detected and their kinetics were studied in detail. The doping of P3HT increased due to the electrochemical oxidation and had resulted in a decrease of the film resistance by a few orders of magnitude. Due to localization on the sample various parameter combinations can be studied quantitatively and reproducibly.

1. Introduction

Organic semiconductors combine the properties of semiconductors with the processability of organic molecules. Recently a lot of effort has been put in the optimization of their physical and chemical properties for organic electronics applications [1]. Big effort was put to understand and improve electrical conductivity which is one of the key points in the construction of organic electronic devices. One of the ways to increase the charge conductivity in an organic semiconductor is via doping [1,2]. There are many ways of doping organic materials:

(1) Chemical oxidation (reduction) for p- (n) doping.
(2) Electrochemical oxidation (reduction) for p- (n) doping.
(3) Field induced doping in organic field effect transistors (OFETs).
(4) Photoinduced doping.

Here electrochemical oxidation and/or reduction are of high interest since it provides easy and flexible variation of redox parameters (doping levels). The variety of physical and chemical parameters, which can be characterized during electrochemical studies, led to the development of different *in situ* techniques [3–8]. Different spectroscopic methods used during cyclic voltammetry measurement allow studying optical, vibrational and electrical changes during oxidation–reduction processes in organic semiconductors. However, all of them are important for understanding doping effects and thus the need for different sample structures and overall big quantities of a material is one of the main obstacles. In an attempt to speed up screening of new materials a new approach leys in a strong miniaturization that allows for drastically reducing the required amount of chemicals. This can be realized by employing scanning droplet cell microscopy (SDCM) with respect to its general applicability for all electrochemical methods even including some combined techniques [9–13].

In this paper an adapted scanning droplet cell microscope and its performance for electrochemical characterization of organic semiconductors is presented. Scanning droplet cell microscopy was applied to measure cyclic voltammetry and electrochemical impedance spectroscopy. The measurement area was up to 3.2 mm^2 allowing multiple characterization on a $15 \times 15\ mm^2$ substrate. The necessary amount of the organic material required for the study was less than 1 mg, and less than 1 ml of electrolyte solution was used. This low consumption of the materials together with large amount of reproducible information obtained makes this setup a very promising technique for screening new organic

* Corresponding author. Tel.: +43 732 2468 8700.
E-mail address: achimwalter.hassel@jku.at (A.W. Hassel).

1572-6657/$ - see front matter © 2012 Published by Elsevier B.V.
http://dx.doi.org/10.1016/j.jelechem.2012.11.008

materials. This paper describes in detail the electrochemical redox processes to characterize regioregular poly(3-hexylthiophene), a standard material for organic solar cells. Two clearly separated and fully reversible oxidation peaks were identified and characterized.

2. Experimental

2.1. Reagents and materials

For this study, a soluble derivative of polythiophenes, the regioregular poly(3-hexylthiophene) (98%, Rieke Metals) was used without further purification. The polymer was dissolved in chlorobenzene (99+%, Acros Organics) with a concentration of 10 g L^{-1} and at a later stage it was deposited by spin coating on a single 15 × 15 mm^2 glass/ITO (15 Ω/□, Kintec Co.) substrate. Before coating, the glass substrate was cleaned by sequential sonication in acetone, isopropanol and de-ionized water. The thickness of the P3HT layer was approximately 100 nm. For all electrochemical studies, 0.1 M solution of tetrabutylammonium hexafluorophosphate ($TBAPF_6$, ⩾99%, Fluka Analytical), prepared by dissolving in propylene carbonate (PC, 99.7%, Sigma Aldrich), was used.

2.2. Scanning droplet cell microscopy

For all the electrochemical investigations, a scanning droplet cell microscope with a three electrode configuration was used [14]. This special feature of small area localization in SDCM can be exploited for various studies in thin film combinatorial libraries [15]. Since only a small electrolyte droplet comes in direct contact with the working electrode surface, even on small samples a high number of investigations can easily be done applying various electrochemical techniques. This increases the number of possible measurements on a single sample and decreases the overall amount of organic material (<1 mg) and electrolyte volume (<1 ml) needed. Fig. 1 shows a photograph of the SDCM during an electrochemical measurement. A plastic block is used for fixing the cell body to an XYZ translation stage which is used for moving the tip of the cell to various locations on the sample surface. The sample representing the working electrode (WE) is electrically contacted using a tungsten needle pressed on a small Indium (In) droplet placed on the ITO substrate. This ensures a good stability of the contact over time. The inset of Fig. 1 shows a schematic representation of the SDCM. The cell was built using a tapered glass capillary (Pasteur pipette) for which a tip diameter of 2 mm was achieved by appropriate grinding. At the top part, an electrolyte inlet is provided by using a 1 mm in diameter Teflon tube connected to the inner volume of the cell and isolated from the exterior by using a two component epoxy resin. An Ag/AgCl quasireference electrode (QRE) was prepared by electrodeposition of AgCl in 1 M HCl on an Ag wire 0.5 mm in diameter. The potential of the RE was found to be 0.211 V vs. standard hydrogen electrode (SHE). Further on, in the entire study all the potential values are given as referenced to the SHE. Details about the AgCl electrodeposition are provided elsewhere [16]. The QRE was also inserted into the cell body from the top, keeping a minimum distance to the WE surface (approximately 1 mm) and fixed with epoxy resin. A gold stripe (Wieland Dentaltechnik 99.999%) (2 mm wide) was used as counter electrode (CE) forming a coil at the top part of the glass capillary, where the inner diameter is still large enough for avoiding electrical contact with the RE. The CE was also embedded into the epoxy resin at the top, which in the final stage of the manufacture completely isolated the inner volume of the cell from exterior. A soft silicone gasket was formed on the rim of the SDCM tip by dipping the capillary in liquid silicone followed by drying it under N_2 flow. This procedure ensured the use of the SDCM with a highly reproducible wetted area in the contact mode, when the cell is pressed against the WE surface and the gasket seals the electrolyte inside the cell for avoiding any air contact [17]. This is an important aspect for the electrochemistry of organic materials when non-aqueous electrolytes are used due to the water contamination from the surrounding atmosphere. The reason behind is that non-aqueous electrolytes are preferred due to the large electrochemical window as compared to aqueous electrolytes.

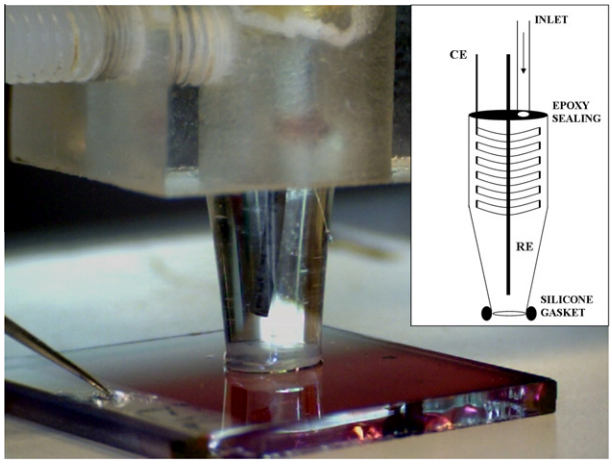

Fig. 1. Photograph and scheme (inset) of the scanning droplet cell microscope (SDCM).

2.3. Electrochemical characterization

All the electrochemical measurements were performed using a combination of a Solartron 1287 potentiostat and a Solartron 1260 frequency response analyzer. Cyclic voltammetry was used for basic characterization of the oxidation of P3HT. For this purpose, the maximum achievable potential was increased from 0 V vs. SHE in steps of 0.05 V up to 1.5 V. Different rates of the potential increase were used ranging between 0.001 V s^{-1} and 0.1 V s^{-1}. Potentiostatic experiments were performed at potentials ranging from 0 V to 1.5 V. Electrochemical impedance spectroscopy (EIS) was used for characterization of the P3HT, by alternating the potentiostatic experiments with impedance measurements. A peak–peak AC perturbation of 0.02 V was applied and the frequency was scanned between 100 kHz and 1 Hz. Mott–Schottky analysis was used for the characterization of the semiconducting properties during doping of P3HT.

3. Results and discussion

3.1. Cyclic voltammetry studies

Fig. 2 shows a series of cyclic voltammograms measured using $TBAPF_6$ electrolyte dissolved in propylene carbonate, with a rate of potential increase of 0.01 V s^{-1}. The maximum achievable potential was increased in 0.05 V steps up to 1.5 V for carefully probing the oxidation and the reduction potentials of the polymer. Two distinct and reversible oxidation potentials were found. The maximum of the first oxidation peak was measured at 0.52 V and the maximum of the second oxidation peak was found at 0.93 V. The reproducibility and stability of the oxidation potentials can be directly analyzed from the CVs shown in Fig. 2. It was found that the first oxidation potential is shifting by 0.1 V during the entire series of investigation. For the second oxidation potential, only a slight shift smaller than 0.1 V was noticed. A constant shifting

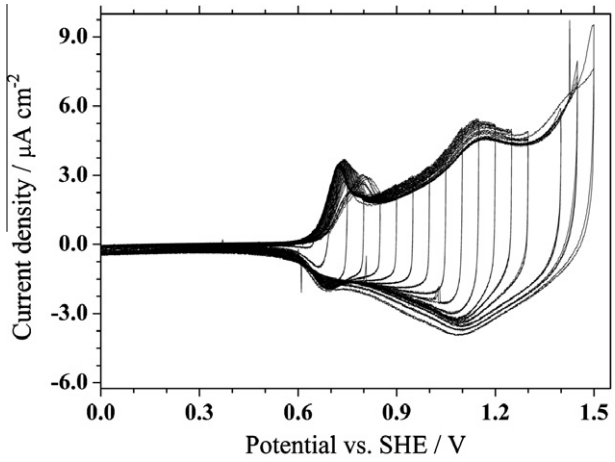

Fig. 2. Cyclic voltammograms of P3HT for various reverse potentials.

might be explained by a not fully reversible oxidation, resulting in a continuous growth of the oxidized polymer layer. In addition, the current density corresponding to the first oxidation peak decreases with approximately 20% during the entire study suggesting a possible decrease of the effective area. This can be attributed to degradation of the electrochemical cell.

In order to study the electrochemical reaction kinetics, cyclic voltammetry with changing scanning rates were used. The SDCM tip was moved to a new location on the surface of the P3HT and scan rates of 1 mV s^{-1}, 3 mV s^{-1}, 10 mV s^{-1}, 30 mV s^{-1} and 100 mV s^{-1} were successively applied. In Fig. 3 these cycles are presented together and a direct comparison between them becomes possible. For each measurement, the current was divided by the scan rate used. The obtained values of dQ/dE as a function of the applied potential in the electrochemical process are presented in Fig. 3. With the increase of the potential scan rate up to 10 mV s^{-1}, the oxidation peaks positions are invariable. For the first three curves, the oxidation peaks are found at 0.52 V and 0.93 V, which are identical with the result obtained previously from Fig. 2. Also, the reduction peaks are found in the same position as before. When further increasing the potential scan rate, the oxidation and reduction peak positions are found to be shifted towards higher respectively lower potentials. The maximum shifts of the oxidation peaks were measured as 0.07 V and 0.05 V corresponding to the first and second peak, respectively. This scan rate dependent measurement gives an insight into the kinetics of the underlying processes. The stronger shift of the first peak with increasing scan rate indicates a stronger kinetic hindrance for this process. Missing an initial conductivity in the fully reduced state does not allow a direct charge penetration whereas this effect is significantly lower for the second peak.

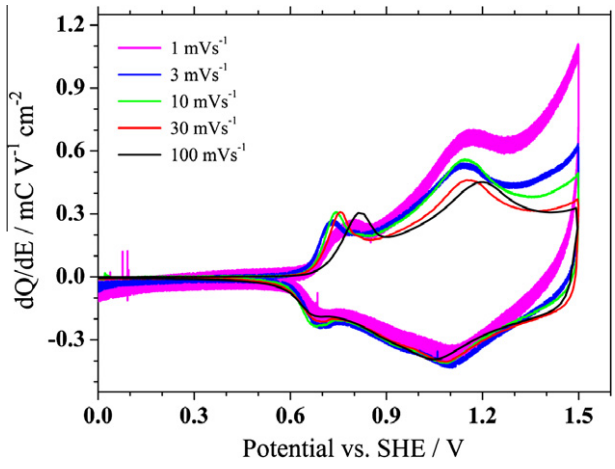

Fig. 3. Scan rate dependent cyclic voltammetric measurements of P3HT.

3.2. Potentiostatic studies

In addition to cyclic voltammetry, a series of potentiostatic experiments was conducted in which the constant potential was increased stepwise in an attempt to determine the oxidation potentials. For the entire measurement series, the layer of P3HT was kept for 10 s at the corresponding potential while the transient current response was measured. These results are presented in the 3D graph of Fig. 4. Differences in the electrochemical processes can be better determined in such series of potentiostatic experiments by an increase in the current, especially when a sufficiently small step of the constant potential is used. For this purpose, a potential increase of 50 mV was found to be suitable. For low potentials, only a background current in the order of 10^{-8} A cm^{-2} could be measured. During the 10 s timeframe for the measurements, this current remains constant. At potentials higher than 0.6 V, the beginning of the current transients shows much higher values than the background level. These values are increasing with the potential from one curve to the next within the series. During the first two seconds, a decrease of the current can be seen. This decrease characterizes the oxidation process of P3HT. Later on, the current stabilizes in plateaus describing the set-in of the electrochemical process equilibrium. The values of the current plateaus are higher than the initial background current and increase with applied potential. This effect might be attributed to an increase in the P3HT conductivity.

The measured current densities after the potentiostatic 10 s pulse can be used for the characterization of the electrochemical processes. All these values are summarized in Fig. 5 for the entire series of potentiostatic experiments. Up to 0.65 V, a constant current density can be observed with a low value in the range of 10^{-8} A cm^{-2}. This value is directly describing the background current of the electrochemical system. Starting from 0.65 V, a first small increase of the current density can be observed, which settles in a first plateau at 4.5×10^{-7} A cm^{-2}. The potential range of this current increase matches the first oxidation peak measured in the CVs from Fig. 2. The first plateau describes the transitional potential range between the first and the second oxidation peaks.

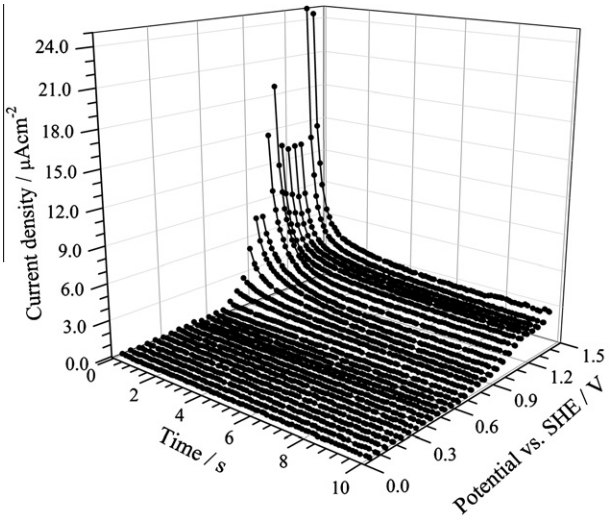

Fig. 4. Time dependent potentiostatic characteristics of P3HT in $TBAPF_6$ electrolyte.

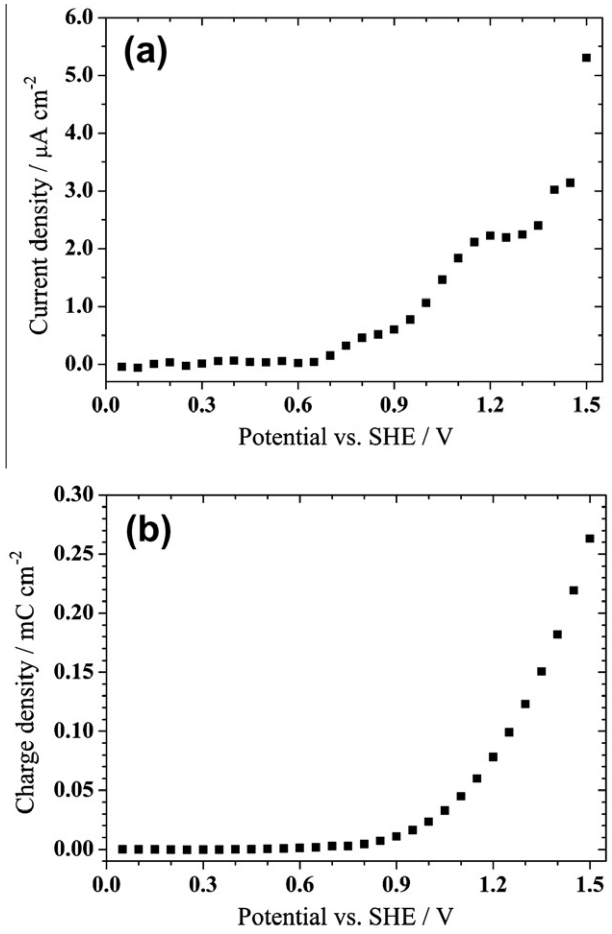

Fig. 5. Analysis of the potentiostatic measurements presenting the current density (a) and charge density (b) as a function of the applied potential.

Above 0.95 V, a second current increase can be observed and the presence of a second current density plateau is revealed starting with 1.2 V. These results fit very well the CVs data presented in Fig. 2. The second current increase characterizes the second oxidation peak, while the second current plateau ends at high potentials where the stability of the system already changes due to various possible degradation processes in the electrolyte, P3HT, ITO or a combination of these factors.

The integration of the potentiostatic transients presented in Fig. 4 combined with their summation allow a description of the total charge consumed up to each potential step during the electrochemical process. In Fig. 5 together with the current densities, the total charge is plotted as a function of the potential. At low potentials up to 0.65 V, the charge level is low, just slightly increasing due to the capacitive charging. Above this potential, a stronger increase of the consumed charge can be observed indicating the start of the oxidation process of the P3HT.

Additionally, more detailed study on the oxidation processes can be done by integrating the potentiostatic currents and subsequently plotting the resulting charge as dQ/dE vs. E for each potential step. Since the charge value is calculated for each potential step after equilibrium is attained, this plot will describe the infinitesimal changes in the electrochemical system. Therefore, it can be interpreted as infinitesimally slow cyclic voltammetry also referred to as quasi stationary measurements. The dQ/dE plot vs. E is presented in Fig. 6. At low potentials up to 0.65 V the amount of charge which takes part in the electrochemical process is low. This is due to the capacitive charging which occurs in the cell.

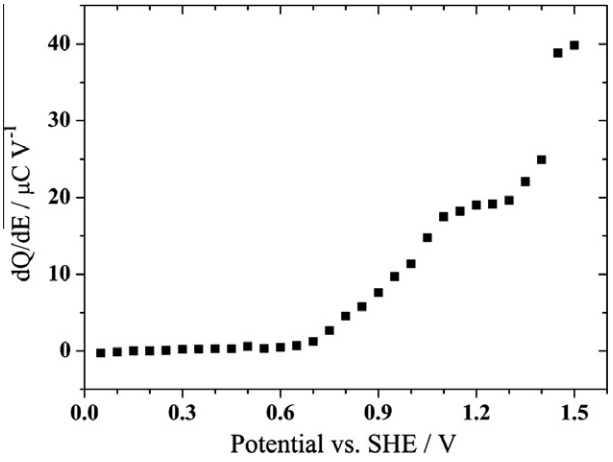

Fig. 6. Charge variation dependence on the applied potential for the P3HT.

Above 0.65 V, an increase in the charge is noticeable since the electrochemical oxidation starts. The slope of the increase can be fitted with two linear functions which describe a double step oxidation process. Above 1.1 V, the values of the dQ/dE reach a plateau which is characterizing the fully oxidized form of the P3HT. Above 1.3 V a further charge increase can be observed. This slope is then representing the degradation processes in the electrochemical cell. In principle the same information would be expected from a CV and a series of potentiostatic current transients. However, the problem with CV can be that a slower process is apparently shifted towards higher potentials and may overlap with a faster process that thermodynamically starts only at higher potentials. In such a case not only an overlap of these two processes would be observed but also an effect may be observed since the second process might then start from a different initial state. A series of potentiostatic pulse experiments in which the final states are plotted against the potential on the other hand does not show this restriction. In case of a coincidence between these experiments is then a clear kinetic proof of applicability.

3.3. Electrochemical impedance spectroscopy

Electrochemical impedance spectroscopy was applied for investigation of the P3HT impedance as a function of the frequency at various potentials. All the measurements were done during the potentiostatic experiment presented in Fig. 4. After each potentiostatic 10 s pulse, necessary for establishing an equilibrium state of the electrochemical process at a given potential, a full impedance spectrum rather than a single frequency measurement was recorded. For each measurement, a bias equal to the constant potential previously used in the potentiostatic experiment was applied. During the entire EIS, the SDCM addressed a single measurement spot. The Bode plots of the impedance spectroscopy on P3HT are presented in Fig. 7. The impedance as a function of the frequency presented in part (a) of Fig. 7 shows a strong dependence on the applied potential. Increasing the bias of the electrochemical process (indicated by the arrow in (a)) resulted in a decrease of the low frequency impedance. This is a direct result of the doping process of P3HT during the electrochemical oxidation which changes the electrical conductivity of the polymeric film [1]. The phase shift recorded during the EIS is presented in part (b) of Fig. 7. The potential increase is again indicated by an arrow and is strongly affecting the measured phase. At low biases, a phase shift of approximately $-75°$ can be observed at frequencies below 1 kHz. Increasing the potential, the phase shift is approaching $-10°$ even at higher frequencies. This behavior can be used for best choosing the

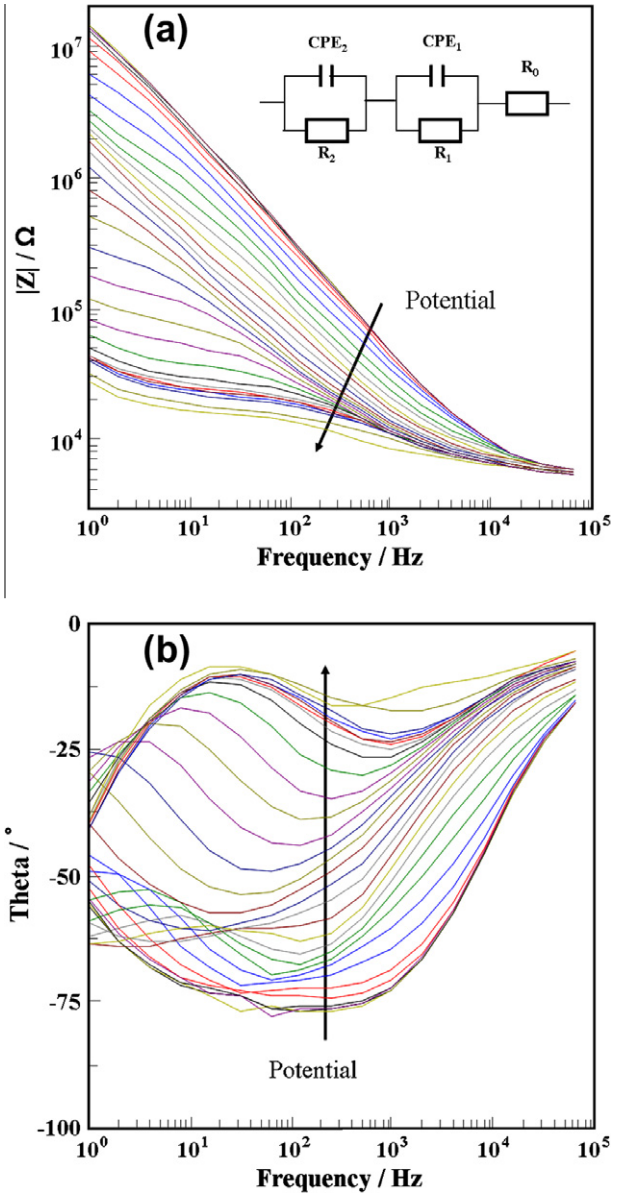

Fig. 7. Bode plots from electrochemical impedance spectroscopy measured in Mott-Schottky regime. The bias was varied between 0 and 1.5 V vs. SHE.

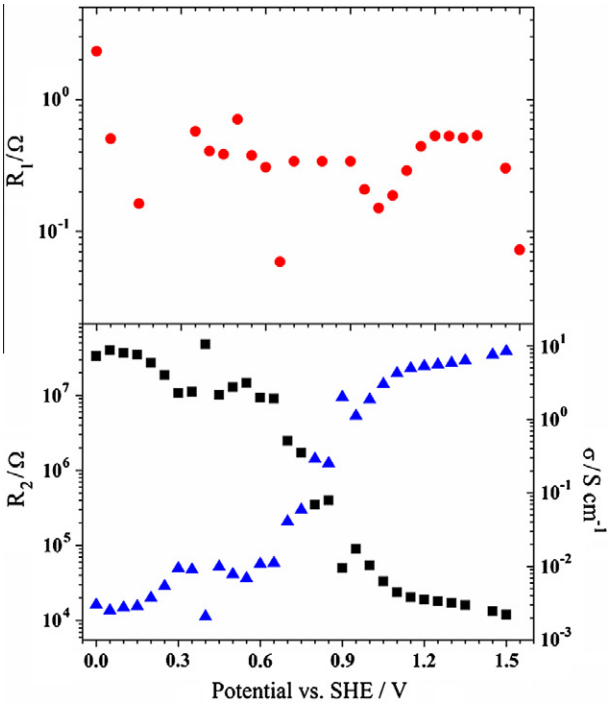

Fig. 8. Comparison of resistances calculated from EIS spectra.

necessary equivalent circuit for fitting all EIS data. The inset of Fig. 7a is depicting the proposed equivalent circuit. For EIS on organic materials, many equivalent circuits were used up to date [18–22]. In the present case, the electrolyte is characterized by a series resistance R_0. This is consistent with all models describing electrochemical processes in conducting electrolytes. The interface between the P3HT film and the bulk electrolyte is characterized by a constant phase element CPE_1 in a parallel configuration with a resistor R_1. This describes the diffuse double layer which forms at the contact between the polymer surface and the electrolyte due to the dipole alignment of adsorbed electrolyte molecules. The CPE_1 simulates a capacitor that is formed by the dipoles, while the R_1 simulates the charge transfer from the electrolyte to the organic layer. The P3HT layer is described by a second parallel circuit formed from another constant phase element CPE_2 and its resistance R_2. The oxidation of the polymer will have as a result the formation of $P3HT^+$ cations which are stabilized by the PF_6^- anions from the electrolyte. This process will influence both values of the R-CPE model used here.

Using the equivalent circuit presented in the inset of Fig. 7a all the measured impedance spectra were fitted using fit software (ZView - Scribner Associates Inc.). In this way, the influence of the separate components of the electrochemical system can be independently analyzed. During the electrochemical process, the value of the electrolyte resistance (R_0) was found to be constant with a value of 5.3 kΩ. Particular interest was given to the values of interface and P3HT layer resistances (R_1 and R_2, respectively). These values are presented in Fig. 8 as a function of the applied potential during the electrochemical process. The interface resistance (R_1) shows an initial decay starting from approximately 2.5 MΩ. This happens during the bias increase up to 0.1 V and the process can be attributed to the dipole alignment of adsorbed electrolyte molecules at the interface. At higher potentials, the interface resistance stabilizes around 400 kΩ slightly fluctuating during the entire potentiostatic analysis up to 1.5 V. The values of the P3HT resistance (R_2) as calculated from the impedance spectra together with the conductivity values are presented in the lower graph from Fig. 8. The change of the polymer layer resistance due to the electrochemical doping is presented as a function of the applied bias. Three distinct regions can be identified. Below 0.65 V a small decrease of the P3HT resistance can be noticed according to the doping of the polymer in contact with electrolyte. This idea is supported by the CVs and the potentiostatic measurements where only background currents were measured. This large film resistance is equivalent with very low film conductivity in the range of mS cm^{-1}. This is expected for undoped or very low doped materials. For higher bias values up to 1.2 V a strong decay by two orders of magnitude of the film resistance are observed. In this potential range both oxidation peaks were found during the cyclic voltammetry (Fig. 3). This region describes a transition to the conducting form of the P3HT and directly characterizes the electrochemical doping of the polymer film. Also, these results can be very well correlated to the current density increase found in the potentiostatic experiments (Fig. 5b) due to the first and second oxidation peaks. In this region the values of conductivity increase by three orders of magnitude reaching 8.4 S cm^{-1}. This value is in full agreement with the previously reported conductivity measurements of

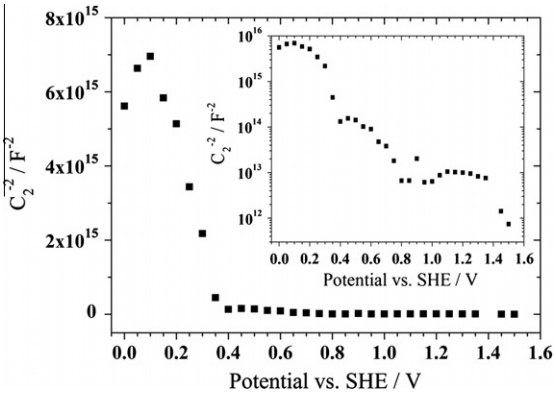

Fig. 9. Mott–Schottky characteristic of P3HT electrochemical doping. The results plotted in the logarithmic scale are presented in the inlet.

the P3HT film after chemical doping in iodine vapor [23] For potentials higher than 1.2 V, the P3HT film resistance showed only a slight decrease indicating the presence of a fully doped state. This result indicates that the final current density increase found during the potentiostatic investigations (Fig. 5b) at potentials above 1.2 V must not be attributed to an electrochemical doping of the P3HT. This statement can be also proven by conductivity calculations were, for potentials above 1.2 V, a plateau is observed. This would rather describe a degradation process of the electrolyte and/or the metallic electrodes.

3.4. Mott–Schottky analysis

For analyzing the semiconducting properties of the P3HT film, Mott–Schottky analysis was conducted during the electrochemical impedance spectroscopy. According to this theory, the inverse square capacitance of a semiconducting layer is proportional to the applied potential [24,25]. In the current study, the conductivity change due to an increase in the doping level is directly reflected in a capacitance change. Therefore, the doping level can be studied qualitatively and quantitatively using this method. The capacitance values of the polymer were determined from CPE_2 measured in the impedance spectra (see Fig. 7) using the equivalent circuit described before. The inverse square capacitance dependence on the applied bias can be followed in Fig. 9. In this figure a drop in the value of the inversed capacitance can be observed above 0.2 V. Since in all experiments, no oxidation processes could be measured up to 0.4 V, this slope describes the semiconducting behavior of the P3HT substrates prior to the electrochemical doping. In this region P3HT has a very low conductivity and still can be described as semiconductor. Using the equation:

$$C_A^{-2} = 2(E - E_{fb} - kT/e)/e\varepsilon\varepsilon_0 N_D \quad (1)$$

where C_A^{-2} is the area normalized inverse square capacitance at certain potential, e is the charge, ε is the P3HT permittivity (in this study 3.5), ε_0 is the vacuum permittivity, E is the applied potential and E_{fb} is the flat band potential, a donor concentration of 1.3×10^{18} cm^{-3} was calculated. This high charge carrier concentration is connected with the air oxygen induced doping [26,27] as well as self-doping of the polymer in contact with electrolyte leading to cation formation. Above 0.4 V the existence of another slope can be noticed as presented in the logarithmic scale in the inlet of Fig. 9. However, since they describe a polymer in the oxidized form which can be treated already as metal, the Mott–Schottky analysis is no longer valid.

4. Conclusions

The electrochemical redox cycles on thin film of P3HT were locally investigated using a modified version of a scanning droplet cell microscopy adapted to organic electrolytes. The possibility of addressing small areas on the surface of the working electrode (3.2 mm^2) combined with the advantage of using low electrolyte volumes (<1 ml) have been exploited in this study. The existence of two oxidation peaks was found during cyclic voltammetry of P3HT and confirmed by further experiments. The electrical behavior of the polymer was characterized *in situ* by electrochemical impedance spectroscopy. A two time constants model was used for fitting the impedance data. An improvement in the electrical conductivity by at least three orders of magnitude was determined. Additionally, Mott–Schottky analysis was employed for determination of the doping level of P3HT.

Acknowledgements

This work is supported by the Austrian Science Foundation (FWF). We gratefully acknowledge Helmut Neugebauer for critically reading the manuscript.

References

[1] A.J. Heeger, N.S. Sariciftci, E.B. Namdas, Semiconducting and Metallic Polymers, Oxford University Press, 2010. 978-0-19-852864-7.
[2] H. Shirakawa, E.J. Louis, A.G. MacDiarmid, C.K. Chiang, A.J. Heeger, J. Chem. Soc., Chem. Commun. (1977) 578–580.
[3] Y. Teketel, S. Lattante, H. Neugebauer, N.S. Sariciftci, M. Andersson, Phys. Chem. Chem. Phys. 11 (2009) 6283–6288.
[4] H. Neugebauer, Macromol. Symp. 94 (1995) 61–73.
[5] P. Meisterle, H. Kuzmany, G. Nauer, Phys. Rev. B 29 (1984) 6008–6011.
[6] S. Klod, F. Ziegs, L. Dunsch, Anal. Chem. 81 (2009) 10262–10267.
[7] A. Petr, L. Dunsch, A. Neudeck, J. Electroanal. Chem. 412 (1996) 153–158.
[8] L. Dunsch, J. Solid State Electrochem. 15 (2011) 1631–1646.
[9] A.L. Whitworth, D. Mandler, P.R. Unwin, Phys. Chem. Chem. Phys 7 (2005) 356–365.
[10] M.A. Edwards, S. Martin, A.L. Whitworth, J.V. Macpherson, P.R. Unwin, Physiol. Meas. 27 (2006) R63–R108.
[11] M.E. Snowden, A.G. Güell, S.C.S. Lai, K. McKelvey, N. Ebejer, M.A. O'Connell, A.W. Colburn, P.R. Unwin, Anal. Chem. 84 (2012) 2483–2491.
[12] S.O. Klemm, J.-C. Schauer, B. Schuhmacher, A.W. Hassel, Electrochim. Acta 56 (2011) 4315–4321.
[13] J.P. Kollender, A.I. Mardare, A.W. Hassel, Chem. Phys. Chem., http://dx.doi.org/10.1002/cphc.201200656.
[14] A.W. Hassel, M.M. Lohrengel, Electrochim. Acta 42 (1997) 3327–3333.
[15] A.I. Mardare, A. Savan, A. Ludwig, A.D. Wieck, A.W. Hassel, Electrochim. Acta 54 (2009) 5973–5980.
[16] A.W. Hassel, K. Fushimi, M. Seo, Electrochem. Commun. 1 (1999) 180–183.
[17] A.I. Mardare, A.W. Hassel, Rev. Sci. Instrum. 80 (2009) 046106.
[18] A. Pitarch, G. Garcia-Belmonte, I. Mora-Seró, J. Bisquert Phys. Chem. Chem. Phys. 6 (2004) 2983–2988.
[19] M. Ates, A. Sezai Sarac, Pol.-Plast. Tech. Eng. 50 (2011) 1130–1148.
[20] J.-S. Yoo, I. Song, J.-H. Lee, S.-M. Park, Anal. Chem. 75 (2003) 3294–3300.
[21] A.-El-H. Bekkali, I. Thurzo, T.U. Kampen, D.R.T. Zahn, Appl. Surf. Sci. 234 (2004) 149–154.
[22] V.S. Reddy, S. Das, S.K. Ray, A. Dhar, J. Phys. D: Appl. Phys. 40 (2007) 7687–7693.
[23] R.D. McCullough, R.D.J. Lowe, J. Chem. Soc. Chem. Commun. 1 (1992) 70–72.
[24] N.F. Mott, Proc. Royal Soc. London A 171 (1939) 27.
[25] W. Schottky, Z. Phys. 113 (1939) 367.
[26] M.S.A. Abdou, F.P. Orfino, Y. Son, S. Holdcroft, J. Am. Chem. Soc. 119 (1997) 4518–4524.
[27] H. Nishimura, M. Iizuka, M. Sakai, M. Nakamura, K. Kudo, Jpn. J. Appl. Phys. 44 (2005) 621–625.